



2D thermo elastic behavior of a FG cylinder under thermomechanical loads using a first order temperature theory



M. Ghannad, M. Parhizkar Yaghoobi^{*}

Faculty of Mechanical Engineering, Shahrood University of Technology, Iran

ARTICLE INFO

Article history:

Received 17 August 2015
Received in revised form
26 November 2016
Accepted 11 December 2016
Available online 12 December 2016

Keywords:

2D thermo elastic
FGM
Cylindrical shell
First order temperature theory
First order shear deformation theory

ABSTRACT

In this paper, steady state thermo-elastic response of axisymmetric FGM cylinder subjected to pressure and external heat flux in inner surface is presented. Displacement field obeys the kinematics of the first order-shear deformation theory (FSDT) and the first order temperature theory is used. Using energy method, the equilibrium equations and general boundary conditions are derived for a cylinder. It is assumed that properties are varied through the thickness by a volume fraction of inner and outer surface properties, using a power law distribution. Based on the developed analytical solution, extensive numerical results are depicted to provide an insight into the influence of the thermal and mechanical loads, boundary conditions and non-homogeneity indices. Results show that shear stress value has noticeable at boundaries and temperature and displacement fields are strongly dependent on length. Furthermore, it is found that the proposed method is robust and accurate for this kind of problem.

© 2016 Elsevier Ltd. All rights reserved.

1. Introduction

Cylindrical shells are extensively used as a structural member in various industries. They have found many applications as load-carrying components in exhaust tubes, pressure vessels, gun tubes, cylindrical tank and etc. Due to the application of cylinders under severe thermo-mechanical loadings, researchers present the idea of functionally gradient material (FGM) to reduce thermal effects in cylinders. The FGM is a nonhomogeneous material whose composition is changed continuously from a metal surface to a ceramic surface. Consequently, it is important to analyze them to promote their reliability and material design. There are a large number of studies in the literature on the static thermo-mechanical analysis of FGM cylindrical shells.

It is worth noting that some investigations have been conducted on the elastic analysis of FGM and homogenous shells [1–12], thermal analysis of FG cylinder is also important and some researcher like [13] deal with Heat Transfer Analysis. For instance, Hongjun et al. [1] presented an analytical solution for elastic

analysis of FGM cylinder based on classic method (Lamé's solution). Same work is conducted by Zhifei et al. [2]. Ghannad and Zamani Nejad [3] through which a closed-form solution for pressurized FGM walled cylindrical shells is presented. The analytical solution is obtained based on the classic method for plane strain and plane stress states. An elasticity solution for thick walled FG cylinder subjected to internal pressure is given by Xin et al. [4]. Their research shows that effects of Poisson ratio variations on the stress and displacement. Considering transverse shear deformation, the elastic analysis of FGM cylinders are presented by the Ghannad and Zamani Nejad [5], based on FSDT formulation. Elastic analyses of cylindrical shells with variable thickness are carried out by Eipakchi et al. [6] and Ghannad et al. [7] for homogenous material and FGM, respectively. Aghdam et al. [8] investigated bending of moderately thick clamped FG conical panels subjected to uniform and nonuniform distributed loadings. FSDT is applied to drive the governing equations of the problem. The governing equations are then solved by the Extended Kantorovich Method. It is also shown that the presented formulation and solution technique can be used to obtain accurate predictions for other types of structures such as circular cylinders and rectangular plates. Xing et al. [9] obtained exact solutions for free vibration of circular cylindrical shells with classical boundary conditions, except for all edges with shear diaphragm. This work is presented those exact solutions based on the Donnell–Mushtari shell theory in simple and compact form. Xin

^{*}Corresponding author. Faculty of Mechanical Engineering, Shahrood University of Technology, P.O. Box 3619995161, Iran.

E-mail addresses: mghannadk@shahroodut.ac.ir, ghannad.mehdi@gmail.com (M. Ghannad), m_parihizkar@shahroodut.ac.ir, m.parihizkaryaghoobi@gmail.com (M. Parhizkar Yaghoobi).

et al. [10] proposed an elasticity solution for the thick-walled FG tube subjected to internal pressure in terms of volume fractions of constituents. The assumption of a uniform strain field is used to obtain governing equation. The closed form solution of the hypergeometric differential equation is given and the corresponding radial displacement and the stresses are presented. Mohammadi-mehr et al. [11] found out the influence of the elastic foundation on the free vibration and buckling of thin-walled piezoelectric-based FGM cylindrical shells under combined loadings. The equations of motion are obtained by using the principle of Hamilton and Maxwell's equations and the Navier's type solution used to solve these equations. In this research, the effects of Pasternak elastic foundation coefficients and also the effects of material distribution, geometrical ratios and loading conditions on the natural frequencies are studied. Zamani Nejad et al. [12] studied semi-analytical a FG rotating thick hollow cylinder with variable thickness and clamped ends under arbitrarily non-uniform pressure on the inner surface. FG cylinder with variable thickness is divided into some homogenous disks; meanwhile some sets of differential equations are obtained based on FSDT for each disk. The solution of this set of equations is obtained, applying the boundary conditions and continuity conditions between the layers, radial displacement and stresses.

The thermo-mechanical studies of cylinders is presented by researchers [14–23] based on classic method. In order to determine the effect of the volumetric ratio of constituents and porosity on thermal stresses, Obata and Noda [14] studied one-dimensional steady thermal stresses in an FG circular hollow cylinder and a hollow sphere by utilizing the perturbation method. Their work indicates that the influence of inner radius size on stresses and the available temperature regions. Zimmerman and Lutz [15] presented solutions for the problem of the uniform heating of a circular cylinder based on Frobenius series method and they found the effective thermal expansion coefficient. Jabbari et al. [16] obtained axisymmetric mechanical and thermal stresses for a hollow cylinder subjected to the temperature and pressure at the inner and outer surfaces. Same work is done by Xin [17] and effect of varying Poisson's ratio is studied. Eslami et al. [18] and Bayat et al. [19] presented the same work for functionally graded sphere. Results of the studies prove that non-homogeneity indices have a substantial effect on stresses and radial displacement distributions in FGM sphere. An analytical solution for the coupled thermoelasticity of cylinders under radial temperature or mechanical shock load is obtained based on the Fourier expansion and Eigen function methods by Jabbari et al. [20]. Seifi [21] found out thermoelasticity behavior of functionally graded thick hollow cylinders with power law and exponential variations of material properties versus radius, analytically. Temperature, displacement, and thermomechanical stress distributions are obtained and discussed. Same work with different method is obtained by Xin et al. [22]. Moosaie [23] investigated a nonlinear thermoelastic analysis of a thick wall cylinder made of functionally graded material. It is assumed the material properties depended on temperature and the perturbation technique is employed to solve the nonlinear heat conduction equation. The so-obtained temperature field is then supplied to elasticity equations which are solved exactly for the case of incompressible elastic material to get displacement and stress distributions.

The thermo-mechanical behavior of cylinder is carried out by Refs. [24–30], by considering shear effect in cylinder. Kim and Noda [24,25] studied the two-dimensional unsteady thermo-elastic problem of a functionally graded infinite hollow cylinder and plate using the Green's function approach. In a later study by

Jabbari et al. [26] non-axisymmetric case of the previous problem was solved using non-axisymmetric temperature distribution by expanding displacements and temperature distribution in the Fourier series. It is worthwhile to note that the aforementioned research [24–26] studied thermo-mechanical behavior in radial and circumferential directions of cylinder. Shao [27] studied the thermo-mechanical stresses of FGM hollow cylinders with the finite length. Results of the study reveal that the proposed method is only suitable for the simply supported boundary conditions and the temperature is zero at two ends. Jabbari et al. [28,29] introduced analytical solutions for two-dimensional and three-dimensional steady-state thermo-elastic problems of the FG circular hollow cylinder, using the generalized Bessel function and Fourier series. Arefi and Rahimi [30] presented an analytical solution for thermo elastic behavior of FGM clamped-clamped cylinder under thermal and mechanical loads based on FSDT. In this case, 1D heat conduction in finite length cylinder through radial direction is considered. Results indicate that there is considerable difference between radial displacement calculated from classic method (1D) and FSDT (2D) analysis. Heydarpour et al. [31] investigated the thermoelastic behavior of rotating laminated FG cylindrical shells in thermal environment. The material properties are assumed to be temperature dependent and graded in the thickness direction. The shell is divided into a set of mathematical layers; the differential quadrature method (DQM) is adopted to discrete the governing differential equations of each layer together with the related boundary and compatibility conditions at the interface of two adjacent layers. Results shows the effects of material and geometrical parameters and also temperature dependence of material properties on the stresses and displacement. Ghorbanpour Arani et al. [32] presented thermo-elastic analysis of a non-axisymmetrically heated FGPM hollow cylinder under multi-physical fields. Material properties is assumed to vary continuously through the thickness. Governing equations are obtained in the form of coupled differential equation sets which are then numerically solved by the DQM to obtain the mechanical behavior in cylinder. Also, static stress analysis of carbon nano-tube which is reinforced by composite cylinder under non-axisymmetric thermo-mechanical loads and uniform electromagnetic fields is presented by Ghorbanpour Arani et al. [33]. Jabbari et al. [34] studied thermo-elastic analysis of axially functionally graded rotating thick cylindrical pressure vessels with variable thickness under mechanical loading. Higher-order shear deformation theory is used to drive the governing equations and it is assumed that the heat conduction occurred only in radial direction. Multi-layer method is applied to solve and the effects of mechanical and thermal loading, thickness profile type, and gradient index on the mechanical behavior of the cylindrical pressure vessel are studied.

The literature survey reveals that analysis of thermo-mechanical loading of a hollow functionally graded cylinder with finite length is less taken into consideration. Also the heat conduction in finite length cylinder is often investigated only in radial direction in these cases, while in real situations the heat conduction can be two dimensional in a finite length cylinder. To the best of the author's knowledge, there is no reported research on the 2D thermo-mechanical analysis of an FG hollow cylindrical shell considering shear effect.

The aim of this paper is to provide an analytical solution to the axisymmetric thermo-mechanical problem of the FG hollow cylinder with finite length which is subjected to pressure and steady-state external heat flux on the inner surface. Material properties of the FG cylinder are varied in the radial direction with a power law function. The temperature, displacement field, and thermal stresses

in the structure under steady state loads are considered. The volume fraction distribution, thermo-mechanical loads, boundary conditions and cylinder geometry are assumed to be axisymmetric. The FGM cylinder results are obtained for the case in which two ends of cylinder are mechanically clamped and they have uniform rise temperature. The effects of material distribution on the temperature, displacements and components of stresses as well as two-dimensional distributions of temperature and displacement field through the cylinder are brought out through a number of parametric studies. The analytical solution which considers arbitrary thermal and mechanical boundary conditions at the two ends of cylinder is used for analysis of the thermal and mechanical behaviors. Using the energy method, the derivation and implementation of an analytical method with its own boundary condition for solving the problems are discussed. The advantage of this method is shown in evaluation of the temperature, displacement and stress fields. The results are consistent with finite element method (FEM).

2. Analysis

A moderately thick-walled cylindrical shell with an inner radius

$$\begin{cases} \varepsilon_z = \frac{\partial U_z(x, z)}{\partial z} = U_z^1(x) \\ \varepsilon_\theta = \frac{U_z(x, z)}{r} = \frac{U_z^0(x)}{R+z} + \frac{U_z^1(x)}{R+z} z \\ \varepsilon_x = \frac{\partial U_x(x, z)}{\partial x} = \frac{dU_x^0(x)}{dx} + \frac{dU_x^1(x)}{dx} z \\ \gamma_{zx} = \frac{\partial U_x(x, z)}{\partial z} + \frac{\partial U_z(x, z)}{\partial x} = \left(U_x^1(x) + \frac{dU_z^0(x)}{dx} \right) + \frac{dU_z^1(x)}{dx} z \end{cases} \quad (2)$$

The thermal field-temperature change relations are

$$\begin{cases} e_z = -\frac{\partial \Theta(x, z)}{\partial z} = -\Theta^1(x) \\ e_x = -\frac{\partial \Theta(x, z)}{\partial x} = -\frac{d\Theta^0(x)}{dx} - \frac{d\Theta^1(x)}{dx} z \end{cases} \quad (3)$$

In addition, the stress tensor and heat flux vector components for isotropic FGMs can be written as

$$\begin{bmatrix} \sigma_z \\ \sigma_\theta \\ \sigma_x \\ \tau_{zx} \end{bmatrix} = \frac{E(z)}{(1-2\nu)(1+\nu)} \begin{bmatrix} 1-\nu & \nu & \nu & 0 \\ \nu & 1-\nu & \nu & 0 \\ \nu & \nu & 1-\nu & 0 \\ 0 & 0 & 0 & \frac{1}{2}(1-2\nu) \end{bmatrix} \begin{bmatrix} \varepsilon_z \\ \varepsilon_\theta \\ \varepsilon_x \\ \gamma_{zx} \end{bmatrix} - \frac{E(z)}{(1-2\nu)} \begin{bmatrix} \alpha(z) \\ \alpha(z) \\ \alpha(z) \\ 0 \end{bmatrix} \Theta \quad (4)$$

$$\begin{bmatrix} h_z \\ h_x \end{bmatrix} = \begin{bmatrix} k(z) & 0 \\ 0 & k(z) \end{bmatrix} \begin{bmatrix} e_z \\ e_x \end{bmatrix}$$

r_i and outer radius r_o , and length L , which is subjected to axisymmetric conditions of pressure P , external heat flux H_i at inner surface, and heat flux H_o at from outer surface to surrounding ambient is considered, Fig. 1.

In this figure, the location of typical point m , (r) within the cylindrical shell element may be determined by R and z , as $r = R + z$ where R represents the distance of middle surface from the axial direction, z is the distance of typical point from the middle surface. It is worth recalling that, z and x must be within the range of $-h/2 \leq z \leq h/2$ & $0 \leq x \leq L$, where h is the thickness of cylinder.

Displacement field (U_z , U_x) and temperature change from reference temperature ($\Theta = T - T^*$) are assumed to be function of z or r and x , which are expressed in the FSDT, as follows ([7,35])

$$\begin{aligned} U_z(x, z) &= U_z^0(x) + U_z^1(x)z, \quad U_\theta(x, z) = 0, \quad U_x(x, z) \\ &= U_x^0(x) + U_x^1(x)z \quad \text{and} \quad \Theta(x, z) = \Theta^0(x) + \Theta^1(x)z \end{aligned} \quad (1)$$

where $U_z^0(x)$ and $U_x^0(x)$ are the displacement components and $\Theta^0(x)$ is the temperature change of the middle surface. Also $U_z^1(x)$, $U_x^1(x)$ and $\Theta^1(x)$ are the functions used to determine the displacement and temperature change field.

The strain-displacement relations (kinematic equations) are

Where σ_i , ε_i , h_i and e_i are the components of stress tensor, strain tensor, heat flux vector and, thermal field vector in the axial (x), circumferential (θ) and radial (z) direction, (τ_{zx} is the shear stress). In the relations (4) $E(z)$, ν , $\alpha(z)$, and $k(z)$ are modulus of elasticity, Poisson's ratio, coefficient of thermal expansion, and thermal conduction coefficient, respectively. Also the value of effective stress based on von Mises failure theory is

$$\sigma_{eff} = \frac{1}{\sqrt{2}} \left[(\sigma_z - \sigma_\theta)^2 + (\sigma_\theta - \sigma_x)^2 + (\sigma_z - \sigma_x)^2 + 6\tau_{zx}^2 \right]^{0.5} \quad (5)$$

The material properties are assumed to be described with the power law as

$$\begin{aligned} E(z) &= (E_o - E_i) \left(\frac{1}{2} + \frac{z}{h} \right)^n + E_i \\ \alpha(z) &= (\alpha_o - \alpha_i) \left(\frac{1}{2} + \frac{z}{h} \right)^n + \alpha_i \\ k(z) &= (k_o - k_i) \left(\frac{1}{2} + \frac{z}{h} \right)^n + k_i \end{aligned} \quad (6)$$

where the volume fraction index n obeys the simple rule of mixture and represents the material variation profiles through thickness, and indices i and o are abbreviations of inner and outer surface,

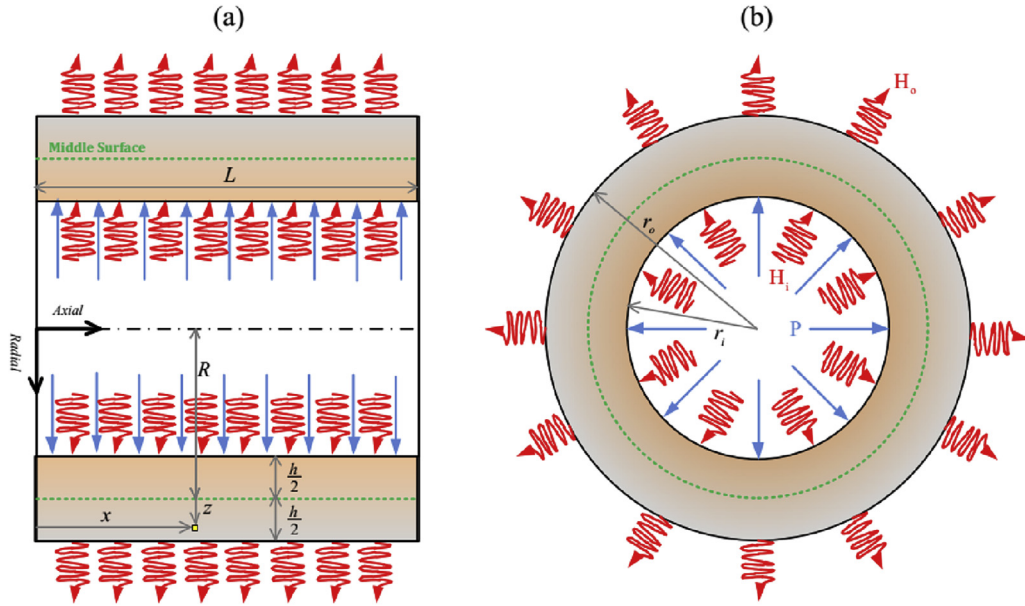


Fig. 1. Cross section of the moderately thick-walled cylinder under thermo-mechanical loading.

respectively. It is assumed that the Poisson's ratio is constant across the shell thickness.

The mechanical and thermal resultants defined as

$$\begin{Bmatrix} N_z^m \\ N_\theta^m \\ N_x^m \end{Bmatrix} = \int_{-h/2}^{h/2} \begin{Bmatrix} \sigma_z \left(1 + \frac{z}{R}\right) \\ \sigma_\theta \\ \sigma_x \left(1 + \frac{z}{R}\right) \end{Bmatrix} dz \quad (7)$$

$$\begin{Bmatrix} M_\theta^m \\ M_x^m \end{Bmatrix} = \int_{-h/2}^{h/2} \begin{Bmatrix} \sigma_\theta \\ \sigma_x \left(1 + \frac{z}{R}\right) \end{Bmatrix} z dz \quad (8)$$

$$\begin{Bmatrix} Q_x^m \\ M_{zx}^m \end{Bmatrix} = \int_{-h/2}^{h/2} \begin{Bmatrix} 1 \\ z \end{Bmatrix} \tau_{zx} \left(1 + \frac{z}{R}\right) dz \quad (9)$$

$$\begin{Bmatrix} N_z^t \\ N_x^t \end{Bmatrix} = \int_{-h/2}^{h/2} \begin{Bmatrix} h_z \\ h_x \end{Bmatrix} \left(1 + \frac{z}{R}\right) dz \quad (10)$$

$$M_x^t = \int_{-h/2}^{h/2} h_x \left(1 + \frac{z}{R}\right) z dz \quad (11)$$

Based on the virtual work principle, the variations of thermo-mechanical potential energy are equal to the variation of the external thermo-mechanical work $\delta U = \delta W$; where U is the total thermo-mechanical potential energy and W is the total external work due to internal pressure and external heat flux.

The thermo-mechanical potential energy and the external work can be written as ([36])

$$\begin{cases} U = \iiint_{\Omega} U^* d\Omega; d\Omega = r dr d\theta dx = (R+z) dz d\theta dx \\ U^* = \frac{1}{2} (\sigma_z \varepsilon_z + \sigma_\theta \varepsilon_\theta + \sigma_x \varepsilon_x + \tau_{zx} \gamma_{zx} - h_z e_z - h_x e_x) \end{cases} \quad (12)$$

$$\begin{aligned} W &= \iint_S (P U_z - H_i \Theta + H_o \Theta) dS \\ &= \int_0^L \int_0^{2\pi} ((P U_z - H_i \Theta) r_i + H_o \Theta r_o) d\theta dx \end{aligned} \quad (13)$$

The variation of the thermo-mechanical potential energy and external work are defined as

$$\begin{aligned} \delta U &= \int_0^L \int_0^{2\pi} \int_{-h/2}^{h/2} (\sigma_z \delta \varepsilon_z + \sigma_\theta \delta \varepsilon_\theta + \sigma_x \delta \varepsilon_x + \tau_{zx} \delta \gamma_{zx} - h_z \delta e_z \\ &\quad - h_x \delta e_x) (R+z) dz d\theta dx \\ \delta W &= \int_0^L \int_0^{2\pi} \left((P \delta U_z - H_i \delta \Theta) \left(R - \frac{h}{2}\right) + H_o \delta \Theta \left(R + \frac{h}{2}\right) \right) d\theta dx \end{aligned} \quad (14)$$

Substituting Eqs. (2)–(4) into Eq. (14), and drawing upon calculus of variation and the virtual work principle, by employing some manipulations, the governing equations are obtained as

$$\begin{cases} R \frac{dN_x^m}{dx} = 0 \\ R \left(Q_x^m - \frac{dM_x^m}{dx} \right) = 0 \\ R \left(\frac{N_\theta^m}{R} - \frac{dQ_x^m}{dx} \right) = P \left(R - \frac{h}{2} \right) \\ R \left(\frac{M_\theta^m}{R} + N_z^m - \frac{dM_{xz}^m}{dx} \right) = -P \frac{h}{2} \left(R - \frac{h}{2} \right) \\ R \frac{dN_x^t}{dx} = H_i \left(R - \frac{h}{2} \right) - H_o \left(R + \frac{h}{2} \right) \\ R \left(N_z^t - \frac{dM_x^t}{dx} \right) = H_i \frac{h}{2} \left(R - \frac{h}{2} \right) + H_o \frac{h}{2} \left(R + \frac{h}{2} \right) \end{cases} \quad (15)$$

Also, the boundary conditions are

$$\begin{aligned} & \left[N_x^m \delta U_x^0 + M_x^m \delta U_x^1 + Q_x^m \delta U_z^0 + M_{zx}^m \delta U_z^1 + N_x^t \delta \Theta^0 + M_x^t \delta \Theta^1 \right]_{0,L} \\ & = 0 \end{aligned} \quad (16)$$

$$\tilde{A}^* = \begin{bmatrix} 0 & 0 & 0 & 0 & 0 & 0 \\ 0 & 0 & 0 & \tilde{A}_{24} & 0 & 0 \\ \tilde{A}_{31} & \tilde{A}_{32} & 0 & 0 & 0 & 0 \\ \tilde{A}_{41} & \tilde{A}_{42} & 0 & 0 & 0 & 0 \\ 0 & 0 & 0 & 0 & 0 & 0 \\ 0 & 0 & 0 & 0 & \tilde{A}_{65} & \tilde{A}_{66} \end{bmatrix} \quad (19)$$

$$\tilde{B}^* = \begin{bmatrix} 0 & 0 & 0 & \tilde{B}_{14} & 0 & 0 \\ \tilde{B}_{21} & \tilde{B}_{22} & \tilde{A}_{23} & 0 & \tilde{B}_{25} & \tilde{B}_{26} \\ 0 & 0 & 0 & \tilde{B}_{34} & 0 & 0 \\ 0 & 0 & 0 & \tilde{B}_{44} & 0 & 0 \\ 0 & 0 & 0 & 0 & 0 & 0 \\ 0 & 0 & 0 & 0 & 0 & 0 \end{bmatrix} \quad (20)$$

$$\tilde{C}^* = \begin{bmatrix} \tilde{B}_{11} & \tilde{B}_{12} & \tilde{A}_{13} & 0 & \tilde{B}_{15} & \tilde{B}_{16} \\ 0 & 0 & 0 & \tilde{C}_{24} & 0 & 0 \\ \tilde{C}_{31} & \tilde{C}_{32} & \tilde{B}_{33} & 0 & \tilde{C}_{35} & \tilde{C}_{36} \\ \tilde{C}_{41} & \tilde{C}_{42} & \tilde{B}_{43} & 0 & \tilde{C}_{45} & \tilde{C}_{46} \\ 0 & 0 & 0 & 0 & \tilde{A}_{55} & \tilde{A}_{56} \\ 0 & 0 & 0 & 0 & 0 & \tilde{C}_{66} \end{bmatrix} \quad (21)$$

and \vec{F}^* is new force vector as follow

$$\vec{F}^* = \left\{ K_1 \quad 0 \quad P \left(R - \frac{h}{2} \right) \quad -P \left(R - \frac{h}{2} \right) \frac{h}{2} \quad \left(H_i \left(R - \frac{h}{2} \right) - H_o \left(R + \frac{h}{2} \right) \right) \frac{x^2}{2} + K_2 x + K_3 \quad \frac{h}{2} \left(H_i \left(R - \frac{h}{2} \right) + H_o \left(R + \frac{h}{2} \right) \right) \right\}^T \quad (22)$$

The number of thermal and mechanical resultants aren't equal to the number of equations in relation (15), thus for solving the set of differential Eq. (15) thermal and mechanical are required to be expressed in terms of the components of temperature and displacement field. With substituting Eqs. (2)–(11) into Eq. (15), set of differential Eq. (15) may be rewritten as

$$\begin{cases} \tilde{A} \frac{d^2}{dx^2} \vec{y} + \tilde{B} \frac{d}{dx} \vec{y} + \tilde{C} \vec{y} = \vec{F} \\ \vec{y} = \left\{ U_z^0 \quad U_z^1 \quad U_x^0 \quad U_x^1 \quad \Theta^0 \quad \Theta^1 \right\}^T \end{cases} \quad (17)$$

where $\tilde{A}_{6 \times 6}$, $\tilde{B}_{6 \times 6}$, $\tilde{C}_{6 \times 6}$ are the coefficients matrices, and \vec{F} is force vector. The nonzero components of $\tilde{A}_{6 \times 6}$, $\tilde{B}_{6 \times 6}$, $\tilde{C}_{6 \times 6}$, and \vec{F} are calculated by the relations that are given in Appendix A.

3. Analytical solution

To solve the set of differential Equation (17), the \vec{y} is changed to \vec{y}^* , the set of differential Eq. (17) could be reformulated by integrating the first and five equation in the set of Eq. (15) and can be rewritten as

$$\begin{cases} \tilde{A}^* \frac{d^2}{dx^2} \vec{y}^* + \tilde{B}^* \frac{d}{dx} \vec{y}^* + \tilde{C}^* \vec{y}^* = \vec{F}^* \\ \vec{y}^* = \left\{ U_z^0 \quad U_z^1 \quad \frac{dU_x^0}{dx} \quad U_x^1 \quad \Theta^0 \quad \Theta^1 \right\}^T \end{cases} \quad (18)$$

where $\tilde{A}_{6 \times 6}^*$, $\tilde{B}_{6 \times 6}^*$, $\tilde{C}_{6 \times 6}^*$ are the coefficients matrices, that are new arrangement of $\tilde{A}_{6 \times 6}$, $\tilde{B}_{6 \times 6}$, $\tilde{C}_{6 \times 6}$ as follows

where K_1 , K_2 , and K_3 are constant that are results of integrating. Eq. (18) is a set of linear non-homogenous differential equations with constant coefficients. Defining the differential operator $P(D)$, Eq. (18) is written as

$$\begin{cases} P(D) = \tilde{A}^* D^2 + \tilde{B}^* D + \tilde{C}^* \\ D = \frac{d}{dx}, \quad D^2 = \frac{d^2}{dx^2} \end{cases} \quad (23)$$

Thus

$$P(D) \vec{y}^* = \vec{F}^* \quad (24)$$

The differential Eq. (24) has the solution including general solution for homogeneous case \vec{y}_g^* and particular solution \vec{y}_p^* as follows

$$\vec{y}^* = \vec{y}_g^* + \vec{y}_p^* \quad (25)$$

For the general solution for homogeneous case, $\vec{y}_g^* = \vec{\xi} e^{mx}$ is substituted in $P(D) \vec{y}^* = \vec{0}$,

$$\left(\tilde{A}^* m^2 + \tilde{B}^* m + \tilde{C}^* \right) \vec{\xi} e^{mx} = \vec{0} \quad (26)$$

Eq. (26) is eigenvalue problem for non-trivial solution $e^{mx} \neq 0$, the determinant of coefficient must be considered to be zero.

$$\det \left(\tilde{A}^* m^2 + \tilde{B}^* m + \tilde{C}^* \right) = 0 \quad (27)$$

The result of Eq. (27) is an eight-order polynomial which is a function of m , the solution of which is an 8 eigenvalues m_i . The eigenvalues are 4 pairs of conjugated root. By calculating

eigenvectors ξ_i correspond to eigenvalues, general solution is obtained, the general solution for Eq. (24) is

$$\vec{y}_g^* = \sum_{i=1}^8 C_i \vec{\xi} e^{m_i x} \quad (28)$$

The constants C_i are obtained by applying boundary condition. In Eq. (24), \vec{F} is quadratic polynomial, consequently particular solution is $\vec{y}_p^* = \vec{y}_{p2}^* x^2 + \vec{y}_{p1}^* x + \vec{y}_{p0}^*$ that \vec{y}_{p2}^* , \vec{y}_{p1}^* & \vec{y}_{p0}^* are unknown coefficients vectors which are obtained by substituting particular solution in Eq. (24).

As a result, the solution is

$$\vec{y}^* = \sum_{i=1}^8 C_i \vec{\xi} e^{m_i x} + \vec{y}_{p2}^* x^2 + \vec{y}_{p1}^* x + \vec{y}_{p0}^* \quad (29)$$

There are 11 constants in \vec{y}^* , that 8 number of them are appeared in general solution and 3 number of them are appeared in particular solution. Now by returning to the main problem \vec{y} , because of integrating from $\frac{dU_x^0}{dx}$ in \vec{y}^* , another constant K_4 is appeared. So, there will be 12 constants that are obtained by applying thermo-mechanical boundary conditions at two ends of cylinder.

Essential boundary conditions, natural boundary conditions, and any combination of them can be expressed at the two ends of cylinder as

$$x = 0, L; \vec{y} = \begin{Bmatrix} U_z^0 \\ U_z^1 \\ U_x^0 \\ U_x^1 \\ \Theta^0 \\ \Theta^1 \end{Bmatrix} \text{ or } \begin{Bmatrix} N_x^m \\ M_x^m \\ Q_x^m \\ M_{zx}^m \\ N_x^t \\ M_x^t \end{Bmatrix} \text{ or } \begin{Bmatrix} U_z^0 \text{ or } N_x^m \\ U_z^1 \text{ or } M_x^m \\ U_x^0 \text{ or } Q_x^m \\ U_x^1 \text{ or } M_{zx}^m \\ \Theta^0 \text{ or } N_x^t \\ \Theta^1 \text{ or } M_x^t \end{Bmatrix} \quad (30)$$

For example, when two ends of cylinder are mechanically clamped and have T_e temperature, the boundary conditions (essential boundary conditions) are

$$x = 0, L; \vec{y} = \begin{Bmatrix} U_z^0 \\ U_z^1 \\ U_x^0 \\ U_x^1 \\ \Theta^0 \\ \Theta^1 \end{Bmatrix} = \begin{Bmatrix} 0 \\ 0 \\ 0 \\ 0 \\ T_e - T^* \\ 0 \end{Bmatrix} \quad (31)$$

When two ends of cylinder are mechanically free and are thermally insulated, the boundary conditions (natural boundary conditions) are

$$x = 0, L; \vec{y} = \begin{Bmatrix} N_x^m \\ M_x^m \\ Q_x^m \\ M_{zx}^m \\ N_x^t \\ M_x^t \end{Bmatrix} = \begin{Bmatrix} 0 \\ 0 \\ 0 \\ 0 \\ 0 \\ 0 \end{Bmatrix} \quad (32)$$

When one ends of the cylinder at $x = 0$ is mechanically free and has T_e temperature and the other end of cylinder at $x = L$ is mechanically clamped and is insulated, the boundary conditions (combined boundary conditions) are

$$x = 0 \rightarrow \vec{y} = \begin{Bmatrix} N_x^m \\ M_x^m \\ Q_x^m \\ M_{zx}^m \\ \Theta^0 \\ \Theta^1 \end{Bmatrix} = \begin{Bmatrix} 0 \\ 0 \\ 0 \\ 0 \\ T_e - T^* \\ 0 \end{Bmatrix}; \quad x = L \rightarrow \vec{y} = \begin{Bmatrix} U_z^0 \\ U_z^1 \\ U_x^0 \\ U_x^1 \\ N_x^t \\ M_x^t \end{Bmatrix} = \begin{Bmatrix} 0 \\ 0 \\ 0 \\ 0 \\ 0 \\ 0 \end{Bmatrix} \quad (33)$$

As mentioned before, by applying boundary conditions the analytical solution is obtained. Mathematic operations that are expressed for solving the set of differential equations are done by writing program in MAPLE 13. It should be noted, the merit of this analytical solution is capable of solving various combinations boundary conditions. Furthermore, in this method there is no need to study solution convergence opposite the analytical series solutions [26,27]. Since solution convergence could be computationally expensive, the proposed method is of great importance to reduce computational costs.

Table 1

Material properties of titanium and zirconia.

Metal: Ti–6Al–4V	Ceramic: ZrO ₂
$E = 66.2$ (GPa)	$E = 117.0$ (GPa)
$\nu = 0.3$	$\nu = 0.3$
$\alpha = 10.3 \times 10^{-6}$ (1/°K)	$\alpha = 7.11 \times 10^{-6}$ (1/°K)
$k = 18.1$ (W/m°K)	$k = 2.036$ (W/m°K)

Table 2

Loading and boundary conditions for cylinders.

	Loading			Boundary conditions			
	Thermal		Mechanical	Thermal		Mechanical	
	Inner surface	Outer surface	Inner surface	x = 0	x = L	x = 0	x = L
Cylinder I	H _i = 150 (W/m ²)	H _o = 0 (Insulated)	P = 80 MPa	T = 50 °C	T = 50 °C	Clamped	Clamped
Cylinder II	H _i = 150 (W/m ²)	H _o = 100 (W/m ²)	P = 80 MPa	T = 50 °C	T = 50 °C	Clamped	Clamped
Cylinder III	H _i = 150 (W/m ²)	H _o = 100 (W/m ²)	P = 80 MPa	T = 50 °C	insulated	Clamped	Clamped
Cylinder IV	H _i = 150 (W/m ²)	H _o = 100 (W/m ²)	P = 80 MPa	T = 50 °C	T = 50 °C	Clamped	Free
Cylinder V	H _i = 150 (W/m ²)	H _o = 100 (W/m ²)	P = 80 MPa	T = 50 °C	insulated	Clamped	Free
Cylinder VI	H _i = 150 (W/m ²)	H _o = 100 (W/m ²)	P = 80 MPa	insulated	T = 50 °C	Clamped	Free

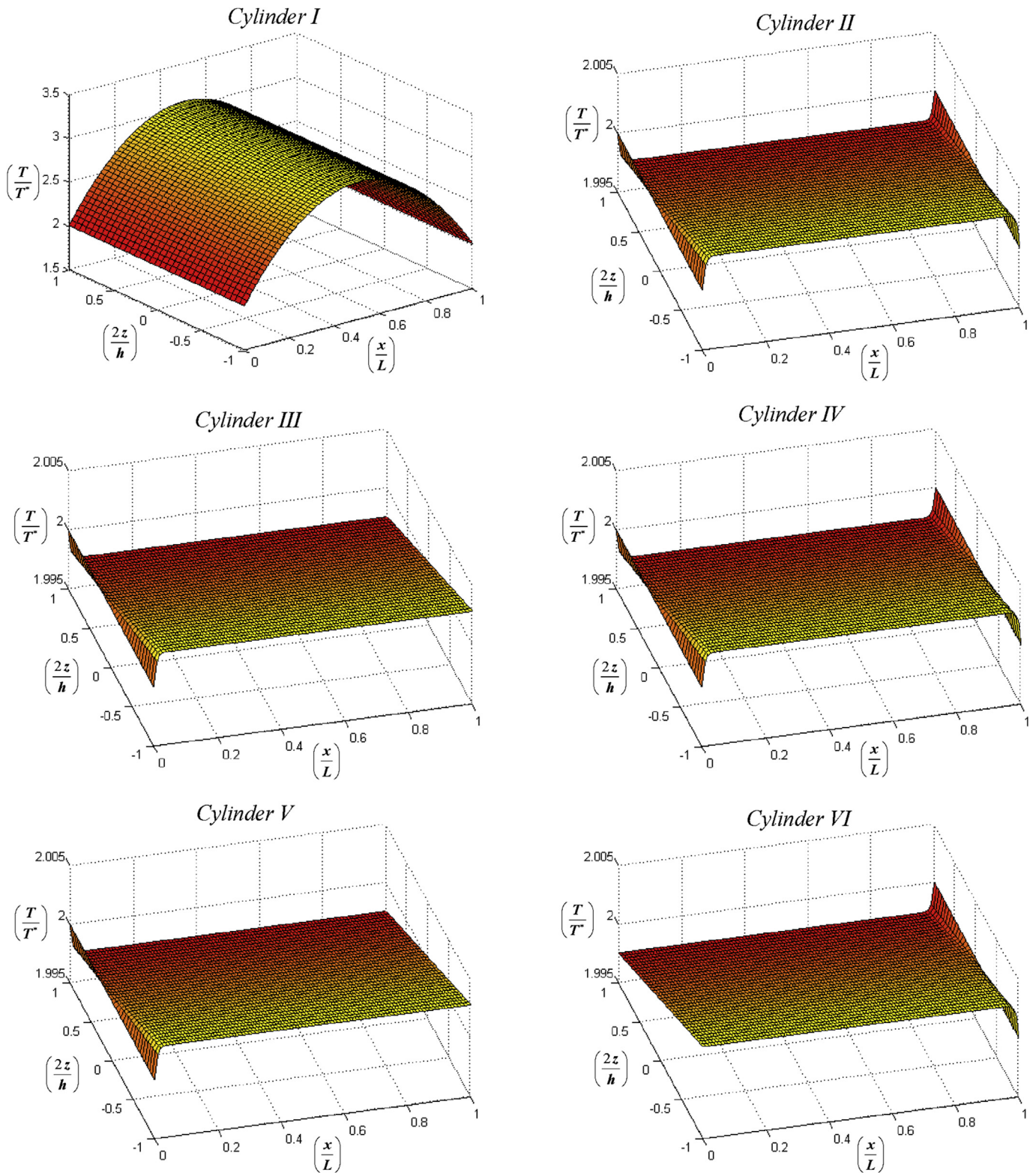


Fig. 2. Distribution of temperature in homogeneous cylinders.

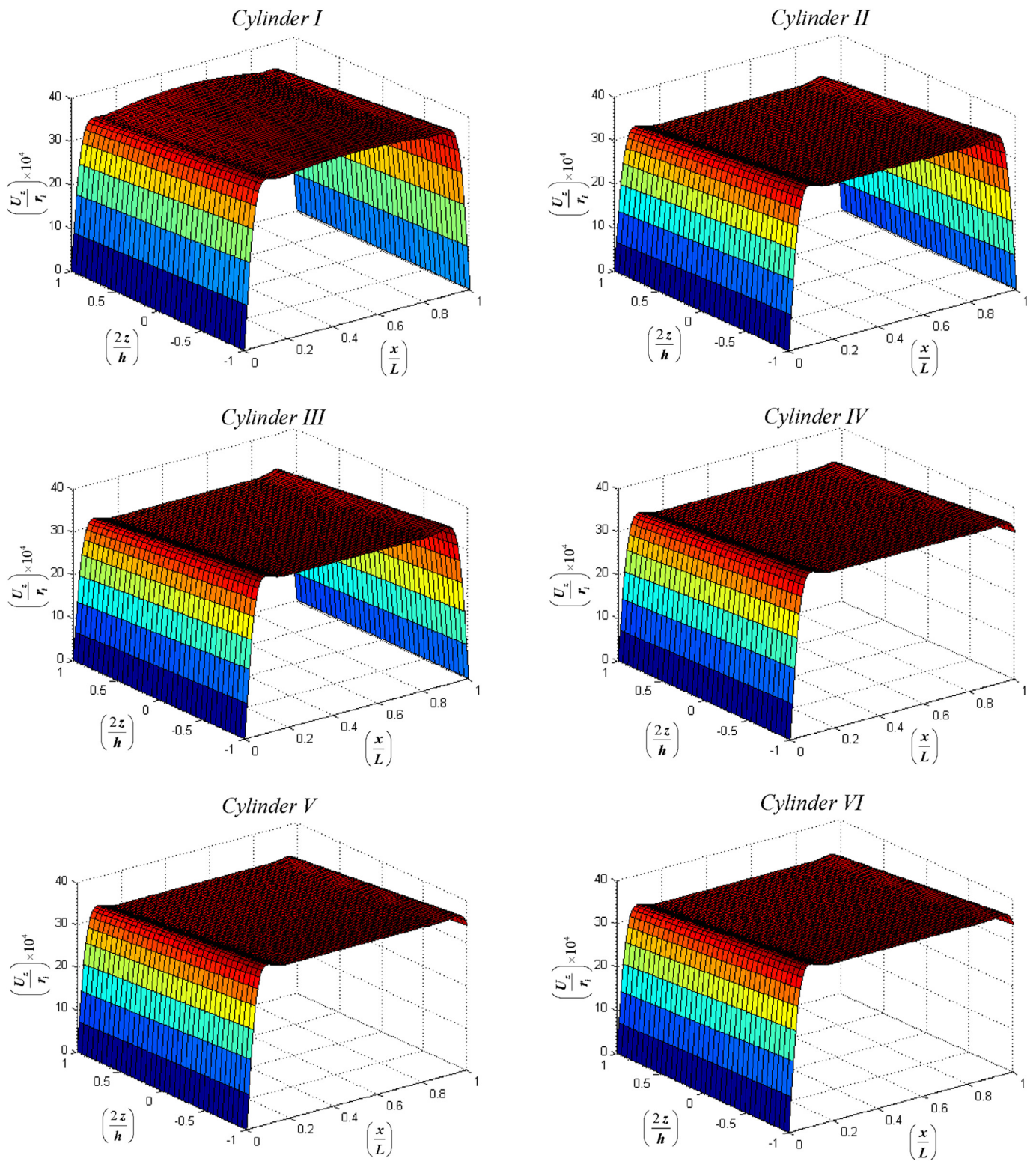


Fig. 3. Distribution of radial displacement in homogeneous cylinders.

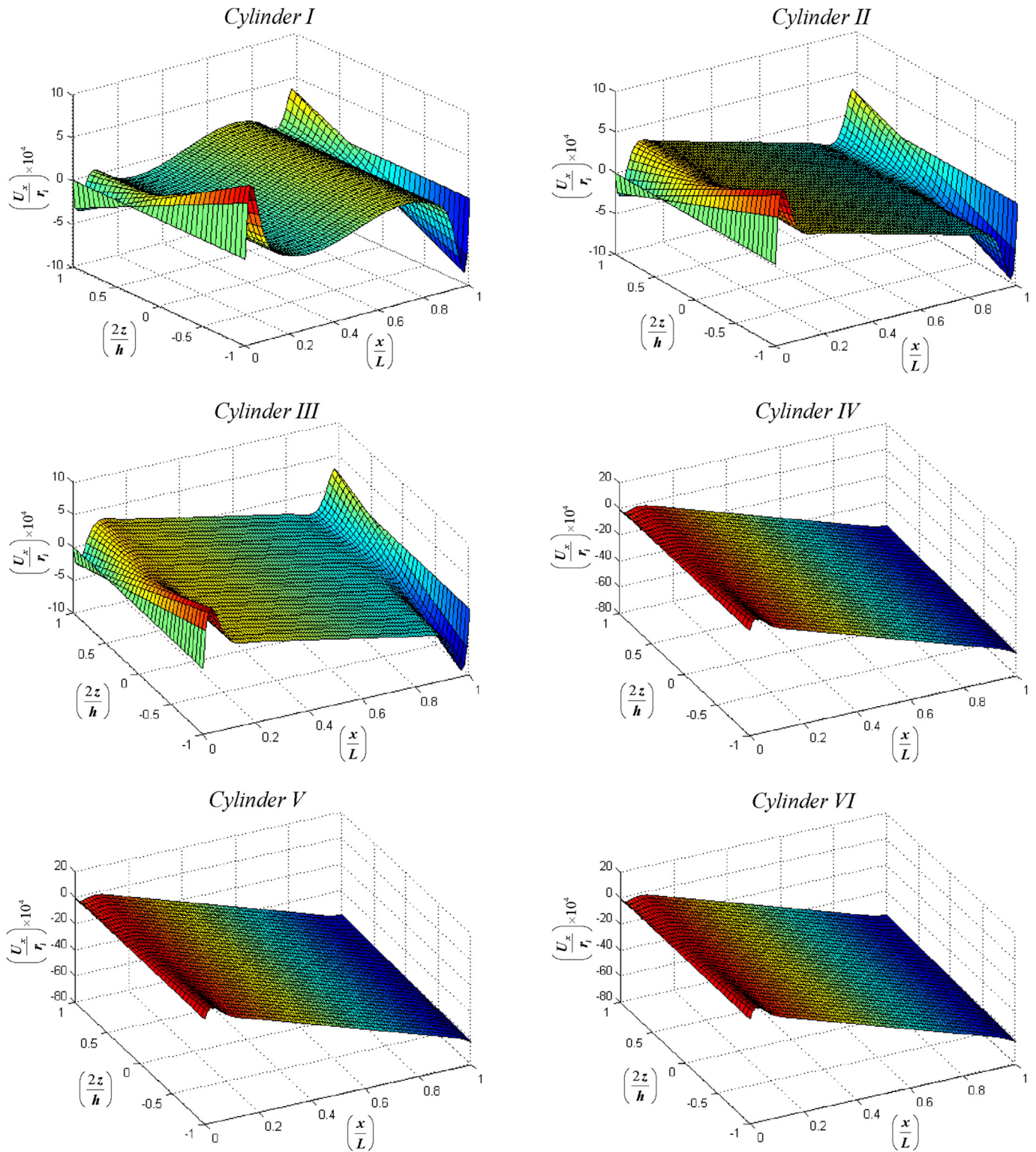


Fig. 4. Distribution of axial displacement in homogeneous cylinders.

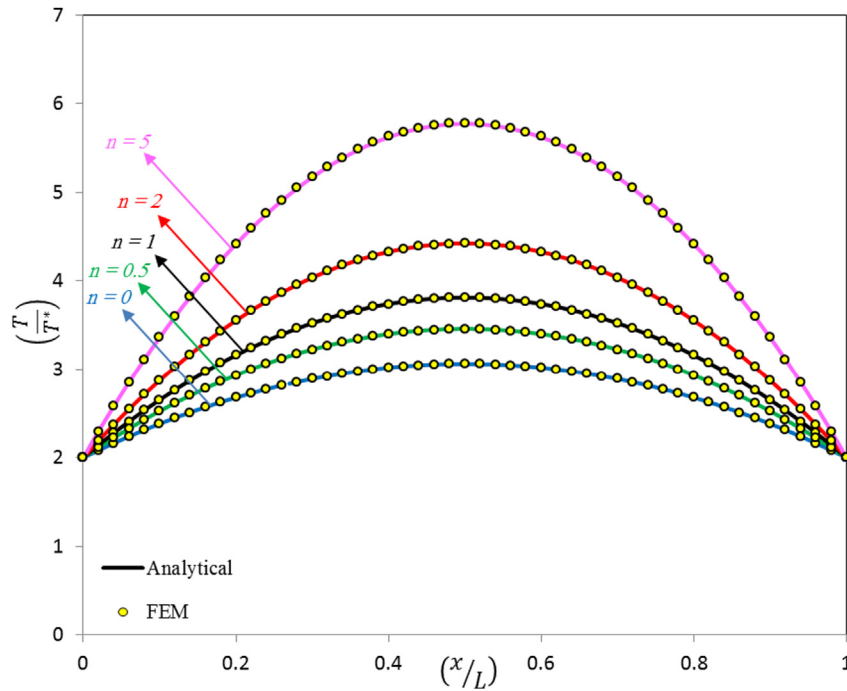


Fig. 5. Distribution of temperature along the middle surface in FGM cylinder I.

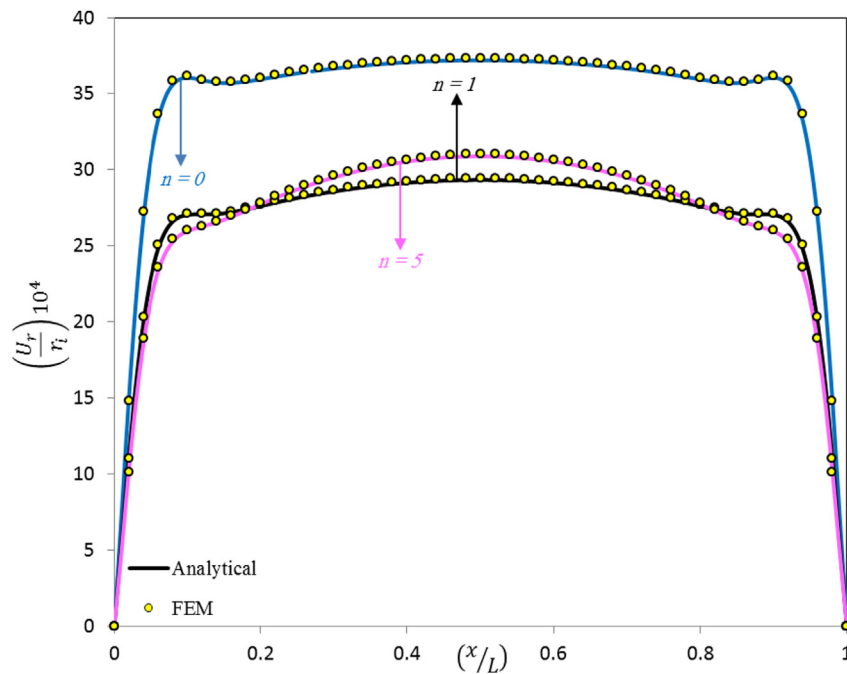


Fig. 6. Distribution of radial displacement along the middle surface in FGM cylinder I.

4. Finite element analysis

The finite element method is a numerical technique to find approximate solutions to boundary value problems for differential equations. For comparative study, case studies are modeled using a commercial FE code, ANSYS. Considering the axisymmetrical conditions, it suffices to select axisymmetric element and model only

the shell section. An axisymmetric element has been used for modeling and meshing. The degrees of freedom are two translations in the radial and axial direction for each node.

In the model, the variation in material properties was implemented by having 20 homogenous layers, with each layer having a constant value of material properties and identical thickness. Properties of each layer are calculated by the following relation.

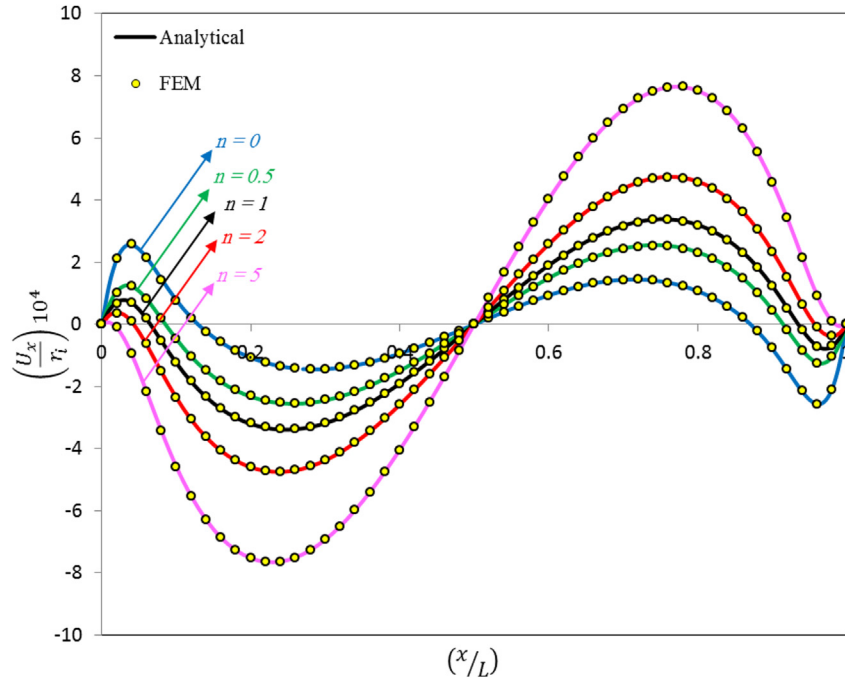


Fig. 7. Distribution of axial displacement along the middle surface in FGM cylinder I.

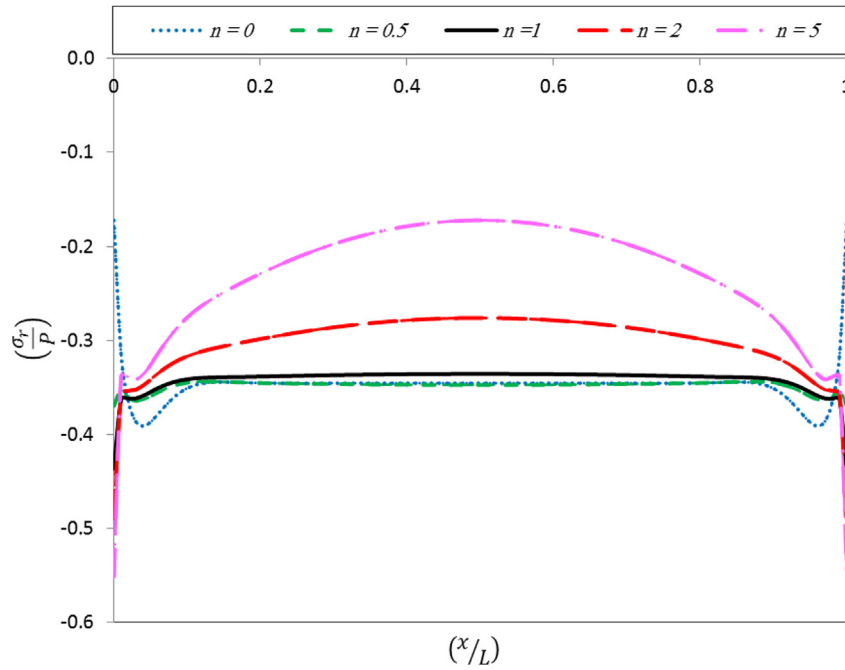


Fig. 8. Distribution of radial stress along the middle surface in FGM cylinder I.

$$E_N = (E_o - E_i) \left(\frac{N}{2} - \frac{1}{40} \right)^n + E_i$$

$$\alpha_N = (\alpha_o - \alpha_i) \left(\frac{N}{2} - \frac{1}{40} \right)^n + \alpha_i$$

$$k_N = (k_o - k_i) \left(\frac{N}{2} - \frac{1}{40} \right)^n + k_i$$

(34)

where N is the number of layers, E_N , α_N and k_N are modulus of elasticity, coefficient of thermal expansion and thermal conduction coefficient of each related layer.

The nodes are subjected to thermal and mechanical loading in inner and outer surface of cylinder elements. Also, based on boundary conditions at two ends of cylinder, nodes at two ends of cylinder are constrained thermally and mechanically.

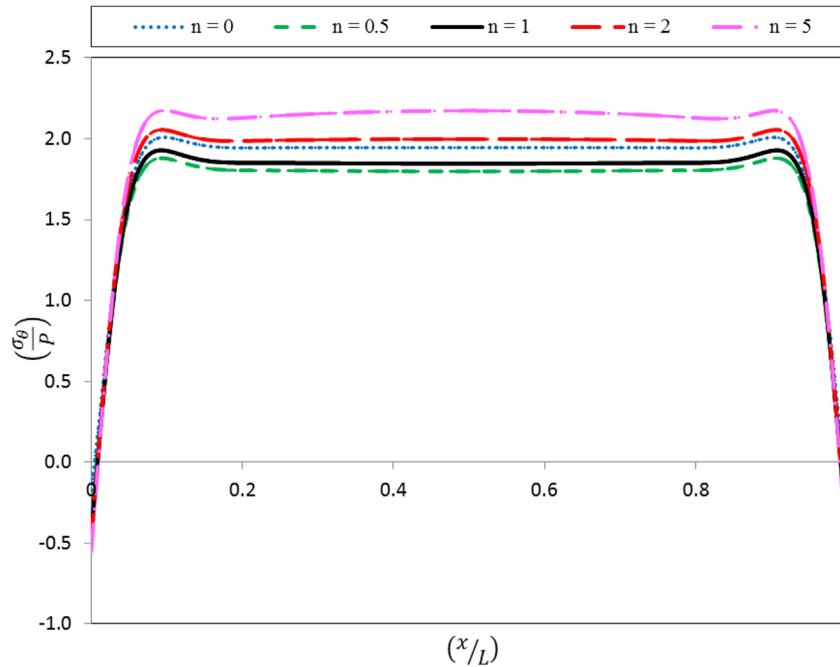


Fig. 9. Distribution of circumferential stress along the middle surface in FGM cylinder I.

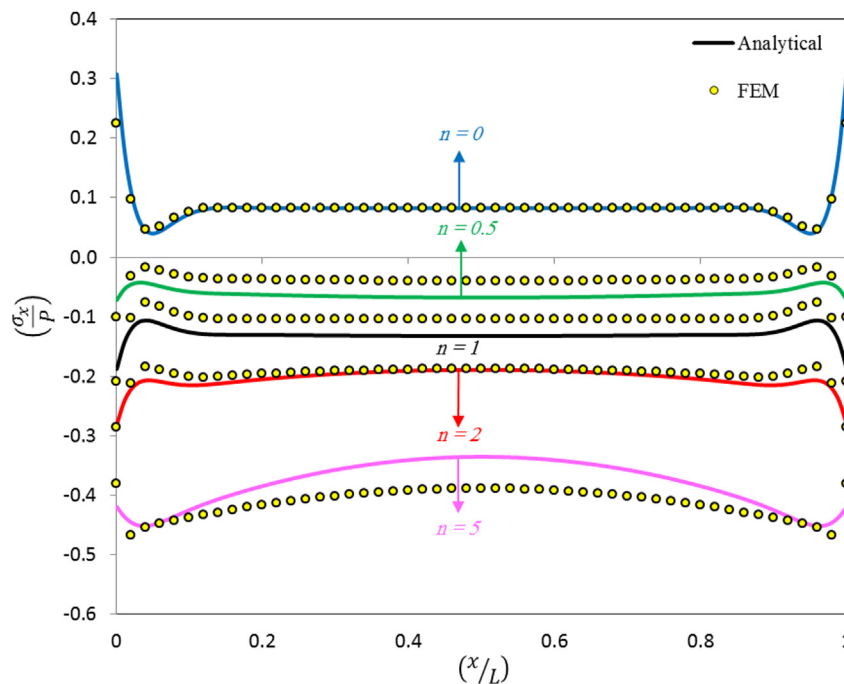


Fig. 10. Distribution of axial stress along the middle surface in FGM cylinder I.

5. Results and discussion

The procedure outlined in the previous section, is implemented herein to study the effect of thermal and mechanical loads and boundary conditions, and inhomogeneity indices on the displacement field, temperature and stresses. To study loading and

boundary conditions, six cylinders with same material and same geometry are considered which are subjected to different thermal loading and boundary conditions. These cylinders with inner radius $r_i = 40 \text{ mm}$, outer radius $r_o = 60 \text{ mm}$ and length $L = 800 \text{ mm}$ are considered. These functionally graded cylindrical shells made of Ti–6Al–4V as metal constituent and ZrO₂ as ceramic constituent

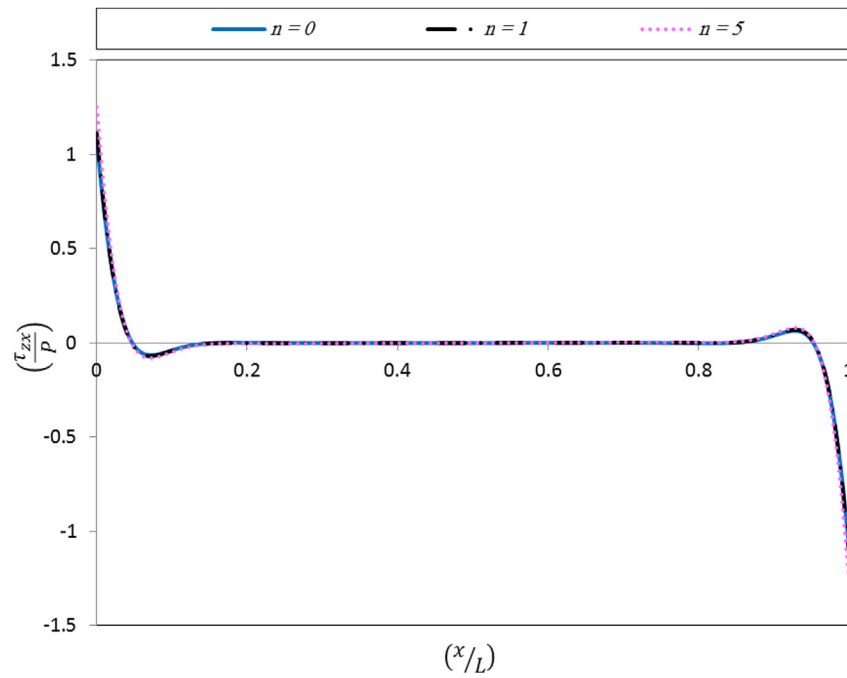


Fig. 11. Distribution of shear stress along the middle surface in FGM cylinder I.

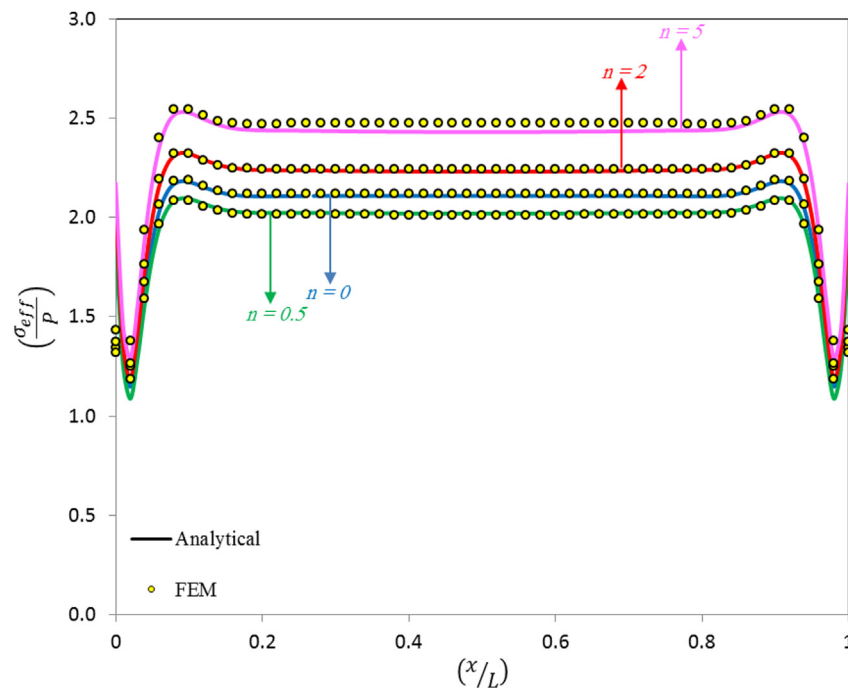


Fig. 12. Distribution of von Mises effective stress along the middle surface in FGM cylinder I.

Table 3

Numerical data from FSDT and FEM calculations for temperature in $x = L/2$.

	T (°C)	n = 0	n = 0.5	n = 1	n = 2	n = 5
Middle surface	FSDT	76.522	86.449	95.292	110.603	144.275
	FEM	76.515	86.417	95.279	110.610	144.450
Inner surface	FSDT	76.557	86.504	95.366	110.709	144.447
	FEM	76.574	86.558	95.535	111.040	145.030

Table 4

Numerical data from FSDT and FEM calculations for radial displacement in $x = L/2$.

	U _r (mm)	n = 0	n = 0.5	n = 1	n = 2	n = 5
Middle surface	FSDT	0.14884	0.12366	0.11736	0.11582	0.12359
	FEM	0.14937	0.12422	0.11786	0.11629	0.12416
Inner surface	FSDT	0.15506	0.12645	0.11866	0.11533	0.12001
	FEM	0.16021	0.13052	0.12265	0.11942	0.12415

are considered. The material properties of constituent at reference temperature $T^* = 25^\circ\text{C}$, are given in Table 1. These shells are ceramic-rich at the inside and metal-rich at the outside surfaces. Table 2 shows that different loading and boundary conditions are considered for six cylinders. To study effect of non-homogeneity on mechanical and thermal behavior of cylinder, the Cylinder I is considered.

Mechanical and thermal behaviors of homogenous cylinders are depicted in Figs. 2–4. Fig. 2 shows the loading and boundary conditions effect on temperature distribution in the cylinders. When the outer surface of cylinders has thermal interaction with surrounding environment and is not insulated, it can be assumed that the temperature only changes in radial direction in the regions far from ends of cylinder. In this conditions, if the mechanical loading doesn't make shear stress, it could be used the classic method (plane strain solution) for analysis. By the way, in the non-insulated regions near the end of cylinder, the temperature varies along the axial axis and makes shear stress, so the present method should be used to see temperature gradient and shear stress distribution. Fig. 2 illustrates that presented method in this paper has no limitation and it's able to deal with different kind of thermal loading and boundary conditions. Based on this analytical method, it could be defined the equal thermal resistance for various loading and boundary conditions that it could be useful for optimization, engineering purpose and design.

Figs. 3–4 illustrates the remarkable effects of boundary conditions on non-dimensional radial and axial displacements of cylinders. When, heat flows out of the outer layer of the cylinder, the radial and axial displacements of cylinders varies linearly along the length. In these conditions, classic method can be used to predict and analyse the mechanical response of cylinder in the regions that they are far from end of cylinder. These figures indicate that the variations of displacements are abruptly at the near end of the cylinder. Also, when the clamped boundary condition changes to free boundary condition, the maximum axial displacement increase about 20 times with no significant changes maximum radial displacement. Changes of displacements at the near ends, lead to the major strains and stresses. It is interesting to note that the displacement field and temperature of cylinder are strongly dependent on axial and radial directions of cylinder and present method is suitable for exact and appropriate analysis.

Temperature profile and radial and axial displacement are plotted in Figs. 5–7 for different values of n at middle surface of cylinder I. It can be concluded from the figures that the results of the proposed analytical method are in great agreement and correlation with FEM data, as the maximum error between the results is less than 2% based on the analytical results. Fig. 5 shows that any increase of the n , results in increase in the temperature, since the increase of non-homogeneity index makes the heat transfer occur sufficiently and consequently the temperature distribution is increased in cylinder I. As mentioned before, according to external heat flux, the maximum temperature is occurred in the middle length of the cylinder I. Fig. 6 depicts that increase of the n leads to decrease or increase of the radial displacements. Actually, increase of non-homogeneity index increases the strength and thermal expansion of the cylinder I. At the initial value of n the effect of strength increase takes major role and the radial displacement is decreased, then the effect of thermal expansion increases and temperature increase becomes majority with increase in the radial displacement. Fig. 7 shows that the n has a substantial effects on the axial displacement, especially in regions that are near boundaries. It was also concluded that the effect of thermal expansion increases

with major increase in temperature and the axial displacement distribution increases by increase n . It is evident from these figures that both maximum values of distributions of the displacements and temperature are strongly affected by volume fractions indices.

Radial, circumferential, axial, and shear stresses for different values of n are illustrated in Figs. 8–11. The effect of non-homogeneity index on radial stress distribution is considerable in Fig. 8. An increase in n results in an increase in the radial stress at the regions that are adequate far from two ends of the cylinder I. Also, an increase in n makes to increase the variations of radial stress distribution in the axial direction. It can be concluded From Fig. 9 that at the regions that are adequately far from two ends of the cylinder I, the circumferential stress is independent from axial direction. Also n has the same effects as radial displacement; increase of the n leads to decrease or increase of the circumferential stress. Fig. 10 shows that as the n increases, the axial compressive stress increases as well. Actually, by increasing the n the temperature distribution is raised and consequently, the axial stress is increased in cylinder I. Fig. 11 demonstrates that shear stress value is considerable in regions that are near boundaries. It should be noted that effect of boundary conditions on stresses value are remarkable. As Fig. 11 shows the approximate relation of the shear stress to boundary conditions and illustrates the little effect of n on shear stress.

Von Mises effective stress for different values of n is shown in Fig. 12. Good agreement between FEM and analytical results is observed. Fig. 12 shows that n has the same effect as circumferential stress; increase of the n leads to decrease or increase of the von Mises stress. The values of von Mises stress at the two ends of the cylinder I are greater than the stresses at the middle of the cylinder I and in the regions that are adequately far from two ends the von Mises stress of the cylinder I tend to an asymptotic value. Thus, based on the von Mises failure criteria, the failure occurs in the ends of cylinder I because the greater value of Von Mises effective stress.

Tables 3 and 4 show the results for T and U_r in middle and inner surface. The obtained results from two methods were compared and good agreements are found. FSDT predicts radial displacement slightly less than FEM.

Table 5 shows the results for stresses in middle surface. The results that are predicted by FSDT have good agreements with FEM.

6. Conclusions

This paper presents an analytical solution to obtain static thermoelasticity response of axisymmetric FGM cylinder which is subjected to pressure and external heat flux in inner surface. Material properties are assumed to be graded along the radial direction according to a power law function. Using energy method and the first-order shear deformation theory, the mechanical and thermal equilibrium equations are derived. The system of differential equations is solved analytically. Based on the developed the analytical solutions, a set of parametric studies was carried out and the following main results are summarized.

- (1) Comparison between the present results (two-dimensional thermal analysis) with the literature (one dimensional thermal analysis) indicates that the displacement field and temperature are strongly depended on axial direction of cylinder even in regions that are far from two ends of cylinder. This difference implies that a two dimensional analysis is inevitable for analysis of the cylinders with finite length.

Table 5Numerical data from FSDT and FEM calculations for stresses in $x = L/2$ & $z = 0$.

	Method	n = 0	n = 0.5	n = 1	n = 2	n = 5
σ_θ (Mpa)	FSDT	155.62	143.90	147.72	159.84	173.85
	FEM	156.15	146.85	150.67	160.67	170.47
σ_x (Mpa)	FSDT	6.60	−5.42	−10.59	−15.13	−26.84
	FEM	6.61	−3.20	−8.35	−15.00	−31.12
σ_{eff} (Mpa)	FSDT	168.76	161.67	167.03	178.55	194.49
	FEM	169.61	161.06	166.43	179.48	198.23

- (2) The advantage of this method is its mathematical power to handle arbitrary boundary conditions at the two ends of cylinder for the static axisymmetric thermo-mechanical analysis of cylinder with finite length. The proposed method may be extended to other kinds of mechanical and thermo-mechanical problems. In addition, this method does not need to study solution convergence opposite the analytical series solutions that are reported in literature.
- (3) This method is suitable for modeling and studying the effect of the ends of cylinder condition; especially the effect of shear deformations and temperature gradients at the two ends of the cylinder. These shear deformations tend to significant gradient of displacement and consequently significant shear stress. Both deformations and stresses can be useful in analysis and design of the cylindrical pressure vessels.
- (4) As the result shows, when the outer surface of cylinder is insulated, the temperature distribution in the cylinder reaches the maximum value and is strongly dependent on axial direction. Under these conditions, the internal axial forces in cylinder increases and increases the axial stress. So, if for the energy consumption considerations, the outer surface are insulated, it should be noted by this work, the axial stresses in the cylinder are grown and even insulated the outer surface of cylinder makes cylinder to buckle.
- (5) Different kinds of thermal and mechanical boundary conditions are studied. Results show that when the mechanical boundary condition changes from clamped to free, the axial displacement of thick cylinder increase significantly but the radial displacement changes is little and they can be ignored.
- (6) Results show that inhomogeneity can change the mechanical and thermal behaviors significantly. The analysis shows that when the power law indices are identical for the modulus of elasticity, coefficient of thermal expansion and the coefficient of conduction the temperature and radial stress increase as the power law index is increased. It is also possible to find an optimum value for inhomogeneity constant such that the variation of stresses and temperature in cylinder is minimized and can be uses for the design.
- (7) Results show that the value of von Mises stresses at the two ends of the cylinder are very greater than the von Mises stresses at the middle of the cylinder. Based on von Mises failure theory, these stresses tend to local yielding at the end of cylinder. Also the present results can be applied for calculation of stress concentration factor due to end supports.

Appendix A

The nonzero components of \tilde{A} are calculated as follows

$$\left\{ \begin{array}{l} \tilde{A}_{13} = \int_{-h/2}^{h/2} \frac{(1-\nu)E(z)}{(1-2\nu)(1+\nu)} (R+z) dz, \quad \tilde{A}_{14} = \int_{-h/2}^{h/2} \frac{(1-\nu)E(z)}{(1-2\nu)(1+\nu)} (R+z)z dz \\ \tilde{A}_{23} = - \int_{-h/2}^{h/2} \frac{(1-\nu)E(z)}{(1-2\nu)(1+\nu)} (R+z)z dz, \quad \tilde{A}_{24} = - \int_{-h/2}^{h/2} \frac{(1-\nu)E(z)}{(1-2\nu)(1+\nu)} (R+z)z^2 dz \\ \tilde{A}_{31} = - \int_{-h/2}^{h/2} \frac{KE(z)}{2(1+\nu)} (R+z) dz, \quad \tilde{A}_{32} = - \int_{-h/2}^{h/2} \frac{KE(z)}{2(1+\nu)} (R+z)z dz \\ \tilde{A}_{41} = - \int_{-h/2}^{h/2} \frac{KE(z)}{2(1+\nu)} (R+z)z dz, \quad \tilde{A}_{42} = - \int_{-h/2}^{h/2} \frac{KE(z)}{2(1+\nu)} (R+z)z^2 dz \\ \tilde{A}_{55} = - \int_{-h/2}^{h/2} k(z)(R+z) dz, \quad \tilde{A}_{56} = - \int_{-h/2}^{h/2} k(z)(R+z)z dz \\ \tilde{A}_{65} = \int_{-h/2}^{h/2} k(z)(R+z)z dz, \quad \tilde{A}_{66} = \int_{-h/2}^{h/2} k(z)(R+z)z^2 dz \end{array} \right. \quad \text{A.1}$$

where K is the shear correction factor that is embedded in the shear stress term. It is assumed that in the static state, for cylindrical shells $K = 5/6$ [4]. Also the nonzero components of \tilde{B} are calculated as follows

The force vector \vec{F} , that is resulting from heat flux and pressure at inner surface are calculated as follows

$$\left\{ \begin{array}{l} \tilde{B}_{11} = \int_{-h/2}^{h/2} \frac{vE(z)}{(1-2v)(1+v)} dz, \quad \tilde{B}_{12} = \int_{-h/2}^{h/2} \frac{vE(z)}{(1-2v)(1+v)} (R+2z) dz \\ \tilde{B}_{15} = - \int_{-h/2}^{h/2} \frac{E(z)\alpha(z)}{(1-2v)} (R+z) dz, \quad \tilde{B}_{16} = - \int_{-h/2}^{h/2} \frac{E(z)\alpha(z)}{(1-2v)} (R+z)z dz \\ \tilde{B}_{21} = \int_{-h/2}^{h/2} \frac{E(z)}{(1+v)} \left(\frac{K(R+z)}{2} - \frac{vz}{(1-2v)} \right) dz, \quad \tilde{B}_{22} = \int_{-h/2}^{h/2} \frac{E(z)}{(1+v)} \left(\frac{K(R+z)}{2} - \frac{v(R+2z)}{(1-2v)} \right) z dz \\ \tilde{B}_{25} = \int_{-h/2}^{h/2} \frac{E(z)\alpha(z)}{(1-2v)} (R+z)z dz, \quad \tilde{B}_{26} = \int_{-h/2}^{h/2} \frac{E(z)\alpha(z)}{(1-2v)} (R+z)z^2 dz \\ \tilde{B}_{33} = \int_{-h/2}^{h/2} \frac{vE(z)}{(1-2v)(1+v)} dz, \quad \tilde{B}_{34} = \int_{-h/2}^{h/2} \frac{E(z)}{(1+v)} \left(\frac{vz}{(1-2v)} - \frac{K(R+z)}{2} \right) dz \\ \tilde{B}_{43} = \int_{-h/2}^{h/2} \frac{vE(z)}{(1-2v)(1+v)} (R+2z) dz, \quad \tilde{B}_{44} = \int_{-h/2}^{h/2} \frac{E(z)}{(1+v)} \left(\frac{v(R+2z)}{(1-2v)} - \frac{K(R+z)}{2} \right) z dz \end{array} \right. \quad \text{A.2}$$

and the nonzero components of \tilde{C} are calculated as follows

$$\left\{ \begin{array}{l} \tilde{C}_{24} = \int_{-h/2}^{h/2} \frac{KE(z)}{2(1+v)} (R+z) dz, \quad \tilde{C}_{31} = \int_{-h/2}^{h/2} \frac{(1-v)E(z)}{(1-2v)(1+v)} (R+z)^{-1} dz \\ \tilde{C}_{32} = \int_{-h/2}^{h/2} \frac{E(z)}{(1+v)(1-2v)} \left(v + \frac{z(1-v)}{(R+z)} \right) dz, \quad \tilde{C}_{35} = - \int_{-h/2}^{h/2} \frac{E(z)\alpha(z)}{(1-2v)} dz \\ \tilde{C}_{36} = - \int_{-h/2}^{h/2} \frac{E(z)\alpha(z)}{(1-2v)} z dz, \quad \tilde{C}_{41} = \int_{-h/2}^{h/2} \frac{E(z)}{(1+v)(1-2v)} \left(\frac{z(1-v)}{(R+z)} + v \right) dz \\ \tilde{C}_{42} = \int_{-h/2}^{h/2} \frac{E(z)}{(1+v)(1-2v)} \left(2vz + (1-v) \left(\frac{z^2}{(R+z)} + (R+z) \right) \right) dz \\ \tilde{C}_{45} = - \int_{-h/2}^{h/2} \frac{E(z)\alpha(z)}{(1-2v)} (R+2z) dz \\ \tilde{C}_{46} = - \int_{-h/2}^{h/2} \frac{E(z)\alpha(z)}{(1-2v)} (R+2z)z dz, \quad \tilde{C}_{66} = - \int_{-h/2}^{h/2} k(z)(R+z) dz \end{array} \right. \quad \text{A.3}$$

$$\vec{F} = \left(R - \frac{h}{2}\right) \left\{ 0 \quad 0 \quad P \quad -P\frac{h}{2} \quad H \quad H\frac{h}{2} \right\}^T \quad A.4$$

List of symbols

r_i	inner radius of cylinder
r_o	outer radius of cylinder
L	length of cylinder
P	internal pressure
H	external heat flux
r	radial coordinate
x	axial coordinate
R	distance of middle surface from the axial coordinate
z	distance from middle surface
h	thickness of cylinder
U_i	displacement components $i = z, x$
T	temperature
T^*	reference temperature
U_i^0	displacement components of the middle surface $i = z, x$
U_i^1	functions used to determine the displacement $i = z, x$
h_i	heat flux components $i = z, x$
e_i	thermal field components $i = z, x$
E	modulus of elasticity
k	thermal conduction coefficient
E_i	modulus of elasticity in internal surface of cylinder
k_i	thermal conduction coefficient in internal surface of cylinder
n_i	inhomogeneity indices $i = 1, 2, 3$
N_i^m, M_i^m, Q_i^m	mechanical resultants $i = z, x, \theta, zx$
N_i^t, M_i^t	thermal resultants $i = z, x$
U	total thermo-mechanical energy
W	external work due to thermo-mechanical load
$\bar{A}, \bar{B}, \bar{C}$	coefficients matrices
\vec{F}	force vector
$\bar{A}^*, \bar{B}^*, \bar{C}^*$	new coefficients matrices
\vec{F}^*	new force vector
K_i	constants of integrating $i = 1, 2, 3$
$P(D)$	differential operator
\bar{y}_g^*	general solution for homogeneous part
\bar{y}_p^*	particular solution
m_i	eigenvalues $i = 1, \dots, 8$
C_i	constants $i = 1, \dots, 8$
\bar{y}_{pi}^*	unknown coefficients vectors $i = 1, 2, 3$

Greek symbols

θ	circumferential coordinate
Θ	temperature change from reference temperature
Θ^0	temperature change of the middle surface
Θ^1	functions used to determine the temperature change
σ_i	stress tensor components $i = z, x, \theta$
τ_{zx}	shear stress
ε_i	strain tensor components $i = z, x, \theta$
γ_{zx}	shear strain
ν	Poisson's ratio
α	coefficient of thermal expansion
α_i	coefficient of thermal expansion in internal surface of cylinder
$\vec{\xi}$	eigenvector

Subscripts

i	inner
o	outer
eff	effective
z	radial direction
x	axial direction
θ	Circumferential direction
p	particular
g	general

Superscripts

m	mechanical
t	thermal
T	transpose

References

- [1] Hongjun X, Zhifei S, Taotao Z. Elastic analyses of heterogeneous hollow cyl-inders. *Mech Res Commun* 2006;33:681–91.
- [2] Zhifei S, Taotao Z, Hongjun X. Exact solutions of heterogeneous elastic hollow cylinders. *Compos Struct* 2007;79:140–7.
- [3] Ghannad M, Zamani Nejad M. Complete elastic solution of pressurized thick cylinder shells made of heterogeneous functionally graded materials. *Mechanika* 2012;18(6):640–9.
- [4] Xin L, Dui G, Yang S, Zhang J. An elasticity solution for functionally graded thick-walled tube subjected to internal pressure. *Int J Mech Sci* 2014;89:344–9.
- [5] Ghannad M, Zamani Nejad M. Elastic analysis of heterogeneous thick cylinders subjected to internal or external pressure using shear deformation theory. *Acta Polytech Hung* 2012;9(6):117–36.
- [6] Eipakchi HR, Rahimi GH, Esmailzadeh Khadem S. Closed form solution for displacements of thick cylinder with varying thickness subjected to non-uniform internal pressure. *Struct Eng Mech* 2003;16(6):731–48.
- [7] Ghannad M, Rahimi GH, Zamani Nejad M. Elastic analysis of pressurized thick cylindrical shells with variable thickness made of functionally graded materials. *Compos Part B-Eng* 2013;45:388–96.
- [8] Aghdam MM, Shahmansouri N, Bigdeli K. Bending analysis of moderately thick functionally graded conical panels. *Compos Struct* 2011;93:1376–84.
- [9] Xing Y, Liu B, Xu T. Exact solutions for free vibration of circular cylindrical shells with classical boundary conditions. *Int J Mech Sci* 2013;75:178–88.
- [10] Xin L, Dui G, Yang S, Zhang J. An elasticity solution for functionally graded thick-walled tube subjected to internal pressure. *Int J Mech Sci* 2013;75:343–9.
- [11] Mohammadimehr M, Moradi M, Loughman A. Influence of the elastic foundation on the free vibration and buckling of thin-walled piezoelectric-based FGM cylindrical shells under combined loadings. *J Solid Mech* 2014;6(4):347–65.
- [12] Zamani Nejad M, Jabbari M, Ghannad M. Elastic analysis of axially functionally graded rotating thick cylinder with variable thickness under non-uniform arbitrarily pressure loading. *Int J Eng Sci* 2015;89:86–99.
- [13] Obata Y, Noda N. Steady thermal stress in hollow circular cylinder and a hollow sphere of functionally gradient materials. *J Therm Stress* 1994;14:471–87.
- [14] Zimmerman RW, Lutz MP. Thermal stresses and thermal expansion in a uniformly heated functionally graded cylinder. *J Therm Stress* 1999;22:177–88.
- [15] Jabbari M, Sohrabpour S, Eslami MR. Mechanical and thermal stresses in a functionally graded hollow cylinder due to radially symmetric loads. *Int J Pres Ves Pip* 2002;79:493–7.
- [16] Xin L, Dui G, Yang S. Solutions for behavior of a functionally graded thick-walled tube subjected to mechanical and thermal loads. *Int J Mech Sci* 2015;98:70–9.
- [17] Eslami MR, Babaei MH, Poultagari R. Thermal and mechanical stresses in a functionally graded thick sphere. *Int J Pres Ves Pip* 2005;82:522–7.
- [18] Bayat Y, Ghannad M, Torabi H. Analytical and Numerical Analysis for the FGM thick sphere under combined pressure and temperature loading. *Arch Appl Mech* 2012;82:229–42.
- [19] M. Jabbari, H. Dehbani, M.R. Eslami, An exact solution for classic coupled thermoelasticity in cylindrical coordinates, *J. Press. Vess-T ASME*, vol. 133, pp. 051204 (10 pages), 2011.
- [20] Seifi R. Exact and approximate solutions of thermoelastic stresses in functionally graded cylinders. *J Therm Stress* 2015;38:1163–82.
- [21] Xin L, Dui G, Yang S. Solutions for behavior of a functionally graded thick-walled tube subjected to mechanical and thermal loads. *Int J Mech Sci* 2015;98:70–9.
- [22] Moosaie A. A nonlinear analysis of thermal stresses in an incompressible functionally graded hollow cylinder with temperature-dependent material properties. *Eur J Mech A-Solid* 2016;55:212–20.
- [23] Kim KS, Noda N. Green's function approach to unsteady thermal stresses in an infinite hollow cylinder of functionally graded material. *Acta Mech* 2002;156:

- 145–61.
- [24] Kim KS, Noda N. A Green's function approach to the deflection of a FGM plate under transient thermal loading. *Arch Appl Mech* 2002;72:127–37.
 - [25] Jabbari M, Sohrabpour S, Eslami MR. General solution for mechanical and thermal stresses in a functionally graded hollow cylinder due to non-axisymmetric steady-state loads. *J Appl Mech-T ASME* 2003;70:111–8.
 - [26] Shao ZS. Mechanical and thermal stresses of a functionally graded circular hollow cylinder with finite length. *Int J Pres Ves Pip* 2005;82:155–63.
 - [27] Jabbari M, Bahtui A, Eslami MR. Axisymmetric mechanical and thermal stresses in thick short length FGM cylinders. *Int J Pres Ves Pip* 2009;86:296–306.
 - [28] Jabbari M, Mohazzab AH, Bahtui A, Eslami MR. Analytical solution for three-dimensional stresses in a short length FGM hollow cylinder, *ZAMM-J. Appl Math Mech/z Angew Math Mech* 2007;87(6):413–29.
 - [29] Arefi M, Rahimi GH. The effect of nonhomogeneity and end supports on the thermo elastic behavior of a clamped-clamped FG cylinder under mechanical and thermal loads. *Int J Pres Ves Pip* 2012;96–97:30–7.
 - [30] Heydarpour Y, Malekzadeh P, Golbahar Haghighi MR, Vaghefi M. Thermo-elastic analysis of rotating laminated functionally graded cylindrical shells using layerwise differential quadrature method. *Acta Mech* 2012;223:81–93.
 - [31] Ghorbanpour Arani A, Abdollahian M, Khoddami Maraghi Z. Thermo-elastic analysis of a non-axisymmetrically heated FGPM hollow cylinder under multi-physical fields. *Int J Mech Mat Des* 2015;11(2):157–71.
 - [32] Ghorbanpour Arani A, Haghpourast E, Khoddami Maraghi Z, Amir S. Static stress analysis of carbon nano-tube reinforced composite (CNTRC) cylinder under non-axisymmetric thermo-mechanical loads and uniform electromagnetic fields. *Compos Part B-Eng* 2015;68:136–45.
 - [33] Jabbari M, Zamani Nejad M, Ghannad M. Thermo-elastic analysis of axially functionally graded rotating thick cylindrical pressure vessels with variable thickness under mechanical loading. *Int J Eng Sci* 2015;96:1–18.
 - [34] Malekzadeh P, Golbahar Haghighi MR, Heydarpour Y. Heat transfer analysis of functionally graded hollow cylinders subjected to an axisymmetric moving boundary heat flux. *Numer Heat Tr A-Appl* 2012;61:614–32.
 - [35] WITT FJ. Thermal analysis of cylindrical shells. *Nucl Struct Eng* 1965;1:276–84.
 - [36] Benjeddou A, Andrianarison O. A thermopiezoelectric mixed variational theorem for smart multilayered composites. *Comput Struct* 2005;83:1266–76.